



# Synergistic Antibiofilm Effects of Pseudolaric Acid A Combined with Fluconazole against *Candida albicans* via Inhibition of Adhesion and Yeast-To-Hypha Transition

Bin Zhu,<sup>a</sup> Zhen Li,<sup>a</sup> Hongmei Yin,<sup>a</sup> Jun Hu,<sup>a</sup> Yingjun Xue,<sup>a</sup> Guanyi Zhang,<sup>a</sup> Xin Zheng,<sup>a</sup> Weiqin Chen,<sup>a</sup>  Xiaobo Hu<sup>a</sup>

<sup>a</sup>Department of Laboratory Medicine, Longhua Hospital, Shanghai University of Traditional Chinese Medicine, Shanghai, People's Republic of China

Bin Zhu and Zhen Li contributed equally to this article. Author order was determined by alphabetical order.

**ABSTRACT** *Candida albicans* biofilms are resistant to several clinical antifungal agents. Thus, it is necessary to develop new antibiofilm intervention measures. Pseudolaric acid A (PAA), a diterpenoid mainly derived from the pine bark of *Pseudolarix kaempferi*, has been reported to have an inhibitory effect on *C. albicans*. The primary aim of the current study was to investigate the antibiofilm effect of PAA when combined with fluconazole (FLC) and explore the underlying mechanisms. Biofilm activity was assessed by tetrazolium {XTT [2,3-bis-(2-methoxy-4-nitro-5-sulfophenyl)-2H-tetrazolium-5-carboxanilide salt]} reduction assays. PAA (4  $\mu\text{g}/\text{mL}$ ) combined with FLC (0.5  $\mu\text{g}/\text{mL}$ ) significantly inhibited early, developmental, and mature biofilm formation compared with the effect of PAA or FLC alone ( $P < 0.05$ ). Furthermore, PAA (4  $\mu\text{g}/\text{mL}$ ) combined with FLC (0.5  $\mu\text{g}/\text{mL}$ ) produced a 56% reduction in *C. albicans* biofilm adhesion. The combination of PAA (4  $\mu\text{g}/\text{mL}$ ) and FLC (0.5  $\mu\text{g}/\text{mL}$ ) also performed well in inhibiting yeast-to-hypha transition. Transcriptome analysis using RNA sequencing and quantitative reverse transcription PCR indicated that the PAA-FLC combination treatment produced a strong synergistic inhibitory effect on the expression of genes involved in adhesion (*ALS1*, *ALS4*, and *ALS2*) and yeast-to-hypha transition (*ECE1*, *PRA1*, and *TEC1*). Notably, PAA, rather than FLC, may have a primary role in suppressing the expression of *ALS1*. In conclusion, these findings demonstrate, for the first time, that the combination of PAA and FLC has an improved antibiofilm effect against the formation of *C. albicans* biofilms by inhibiting adhesion and yeast-to-hypha transition; this may provide a novel therapeutic strategy for treating *C. albicans* biofilm-associated infection.

**IMPORTANCE** Biofilms are the primary cause of antibiotic-resistant candida infections associated with medical implants and devices worldwide. Treating biofilm-associated infections is a challenge for clinicians because these infections are intractable and persistent. *Candida albicans* readily forms extensive biofilms on the surface of medical implants and mucosa. In this study, we demonstrated, for the first time, an inhibitory effect of pseudolaric acid A alone and in combination with fluconazole on *C. albicans* biofilms. Moreover, pseudolaric acid A in combination with fluconazole exerted an antibiofilm effect through multiple pathways, including inhibition of yeast-to-hypha transition and adhesion. This research not only provides new insights into the synergistic mechanisms of antifungal drug combinations but also brings new possibilities for addressing *C. albicans* drug resistance.

**KEYWORDS** *Candida albicans*, antibiofilm, fluconazole, pseudolaric acid A, resistance, synergism

*Candida albicans*, a commensal organism, is normally found on the skin and mucous membrane surfaces of humans. However, when the human microbiota is imbalanced and the immune system impaired, *Candida albicans* can become pathogenic and cause

**Editor** Sudha Chaturvedi, Mycology Laboratory, Wadsworth Center

**Copyright** © 2022 Zhu et al. This is an open-access article distributed under the terms of the [Creative Commons Attribution 4.0 International license](https://creativecommons.org/licenses/by/4.0/).

Address correspondence to Xiaobo Hu, [huxiaobo@vip.sina.com](mailto:huxiaobo@vip.sina.com), or Weiqin Chen, [wonderforjune@126.com](mailto:wonderforjune@126.com).

The authors declare no conflict of interest.

**Received** 8 September 2021

**Accepted** 18 February 2022

**Published** 17 March 2022

invasive candidiasis (1). Statistics indicate that at least 250,000 new cases of invasive candidiasis are diagnosed worldwide each year and more than 50,000 people die from invasive candidiasis (2). *Candida albicans* is the most common pathogen causing invasive candidiasis, accounting for 40 to 50% of cases (3). One crucial factor that is conducive to the pathogenesis of invasive *C. albicans* candidiasis is biofilm formation, since *C. albicans* is able to form biofilms readily on both abiotic and biotic surfaces (4). Combating *C. albicans* biofilms requires the use of antifungal drugs. Antifungal drugs used clinically primarily include the polyene drug classes echinocandins and azoles, of which azoles, especially fluconazole (FLC), are most commonly used in the treatment of *C. albicans* infections (5, 6). However, biofilms enable genetic resistance to antifungal drugs, including FLC (7), which makes FLC treatment of *C. albicans* biofilms inefficient. Therefore, there is a critical need to identify new antifungal agents or combination therapies to fight biofilm-related infections.

The utilization of natural products, such as Chinese herbal monomers, offers new prospects for the development of novel drug entities (8). Several phytochemicals have been found to potentially inhibit biofilm formation and, in combination with FLC, exhibit synergistic effects against *C. albicans* biofilms (9). For example, Dong et al. found that a combination of curcumin derivatives and FLC showed synergistic antifungal activity against *C. albicans* biofilm formation (10). Pseudolaric acid A (PAA) is a diterpenoid extracted from a traditional Chinese medicine, the root bark of *Pseudolarix kaempferi*. The root bark of *Pseudolarix*, known as "Tu-Jin-Pi," has long been used for the treatment of skin infections in China (11).

Research suggests that PAA has antifungal activity against *C. albicans* (12). Biofilm formation is one of the primary antifungal mechanisms responsible for the FLC resistance of *C. albicans*. However, to date, there are no published studies of the effects of PAA alone or in combination with FLC against *C. albicans* biofilms, and the specific antibiofilm mechanism has not been fully clarified yet.

The aim of the current study was to evaluate and determine the antibiofilm activity of PAA combined with FLC (PAA-FLC) against *C. albicans*. Furthermore, changes in adherence properties, yeast-to-hypha transition, and the expression levels of specific biofilm-related genes were measured to elucidate the antibiofilm mechanisms of the combination therapy. The ultimate goal of this study was to provide an effective solution to the problem of biofilm-related drug resistance.

## RESULTS

**Effects of PAA or FLC alone against *C. albicans* biofilm formation.** The process of biofilm formation involves various stages, including the early stage (adhesion), the developmental stage (appearance of hypha), and the mature stage (matrix deposition and hyphal elongation). The antibiofilm effects of PAA or FLC at different stages were evaluated by XTT [2,3-bis-(2-methoxy-4-nitro-5-sulfophenyl)-2H-tetrazolium-5-carboxanilide salt] reduction assays. Based on the results of the XTT reduction assays, the percentage of production at different stages of biofilm formation was calculated and compared with that of the untreated control. During the early biofilm phase (1.5 h), both PAA and FLC produced obvious dose-dependent decreases in *C. albicans* biofilm formation. The biofilm formation rates were about 20% in 8  $\mu\text{g}/\text{mL}$  PAA and 23% in 0.25  $\mu\text{g}/\text{mL}$  FLC for *C. albicans* ATCC 90028 (Fig. 1). At the developmental biofilm stage (6 h), PAA or FLC suppressed biofilm formation in a dose-dependent manner; however, the drug concentration required to suppress biofilm formation was higher than that for the early biofilm stage. At 16  $\mu\text{g}/\text{mL}$ , PAA or FLC hindered nearly 80% of biofilm formation by *C. albicans* (Fig. 1). At the mature stage of biofilm formation (24 h), PAA or FLC alone had no significant antibiofilm activity, even at the highest drug concentration (512  $\mu\text{g}/\text{mL}$ ) (Fig. 1). Specifically, the biofilm formation rate of early biofilm at 64  $\mu\text{g}/\text{mL}$  PAA or FLC was less than 20%; however, the biofilm formation rate of mature biofilm was more than 65% at the same concentration.

**Synergism of PAA and FLC against *C. albicans* biofilm formation.** The *in vitro* synergism of PAA in combination with FLC against biofilm formation was examined with checkerboard assays. Compared with the effects of PAA or FLC alone, PAA in

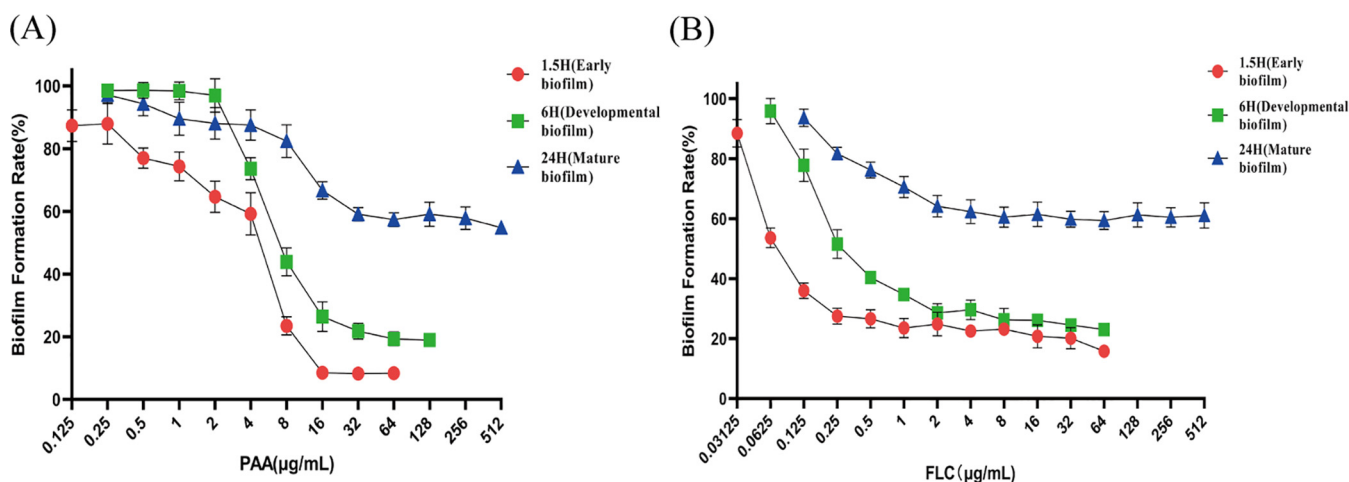


**FIG 1** Effect of PAA or FLC against *C. albicans* biofilm formation at different formation stages. (A) The biofilm formation rate using PAA alone against *C. albicans* biofilm formation at various time points (1.5, 6, and 24 h). (B) The biofilm formation rate using FLC alone against *C. albicans* biofilm formation at various time points (1.5, 6, and 24 h). 1.5, 6, and 24 h relate to the time points of drug treatment during biofilm formation. 1.5 h (early biofilm): *C. albicans* ATCC 90028 cells were allowed to adhere for 1.5 h, and then PAA or FLC alone was added and the cells were incubated for another 24 h at 37°C. 6 h (developmental biofilm): *C. albicans* ATCC 90028 cells were allowed to adhere for 6 h, and then PAA or FLC alone was added and the cells were incubated for a further 24 h at 37°C. 24 h (mature biofilm): after 24 h of cell adherence to form mature biofilms, *C. albicans* ATCC 90028 cells were treated with PAA or FLC alone for an additional 24 h at 37°C. Values represent the means  $\pm$  standard deviation of three replicates.

combination with FLC exhibited a strong inhibitory effect on biofilm formation in the early, developmental, and mature stages of biofilm formation (Fig. 2A to C). In the early and developmental stages of biofilm formation, with increasing doses of PAA and FLC, the synergistic effect against early and developmental biofilm formation was more evident. PAA (4  $\mu\text{g}/\text{mL}$ ) in combination with FLC (0.5  $\mu\text{g}/\text{mL}$ ) showed a significant synergistic effect by reducing biofilm formation by approximately 42% and 49% in the early and developmental biofilm formation stages compared with the reduction observed with 4  $\mu\text{g}/\text{mL}$  PAA alone ( $P < 0.05$ ) (Fig. 2D). At the mature biofilm stage (24 h), the effect of the combination treatment was also found to be stronger than that of PAA or FLC alone. For example, FLC (0.5  $\mu\text{g}/\text{mL}$ ) in combination with PAA at the increasing concentrations of 1, 4, and 32  $\mu\text{g}/\text{mL}$  resulted in reductions in biofilm activity of 73%, 58%, and 43%, respectively (Fig. 2C). Interestingly, treatment with the combination of PAA (4  $\mu\text{g}/\text{mL}$ ) and FLC (0.5  $\mu\text{g}/\text{mL}$ ) significantly inhibited early, developmental, and mature biofilm formation ( $P < 0.05$ ) compared with PAA or FLC alone (Fig. 2D).

**Effects of PAA and FLC on the growth and metabolic activity of biofilms.** The fluorescein diacetate (FDA) method was used to evaluate the growth and metabolic activity of biofilms by observing the number and brightness of fluorescent cells. As shown by the images in Fig. 3, the combination of PAA (4  $\mu\text{g}/\text{mL}$ ) and FLC (0.5  $\mu\text{g}/\text{mL}$ ) significantly reduced the growth and cell activity of biofilms in different stages. Biofilms are highly structured microbial communities that are wrapped by an extracellular polymer matrix (13). In the control group without treatment, dense microbial populations composed of yeast cells and mycelia were observed. When FLC (0.5  $\mu\text{g}/\text{mL}$ ) was combined with PAA (4  $\mu\text{g}/\text{mL}$ ), the numbers of both planktonic cells and hyphae were lower than the numbers in the drug-free control, and the metabolic activity was also weaker than that in biofilms treated with FLC or PAA alone. This result suggests that PAA in combination with FLC decreased the growth and metabolic activity of biofilms in different formation stages, which is consistent with the results of the XTT reduction assays.

**Potential antibiofilm mechanism studies. (i) PAA combined with FLC decreased adhesion of *C. albicans* during biofilm formation.** Since the adhesion of *C. albicans* is the first step in biofilm formation (14), the effects of PAA and FLC on adhesion were observed. The results of the XTT assay revealed that PAA (4  $\mu\text{g}/\text{mL}$ ) in combination with FLC (0.5  $\mu\text{g}/\text{mL}$ ) significantly inhibited biofilm formation. The application of PAA or FLC alone significantly reduced the adhesion rate compared to that in the untreated control; however, the combination of the two drugs further decreased cell adhesion.

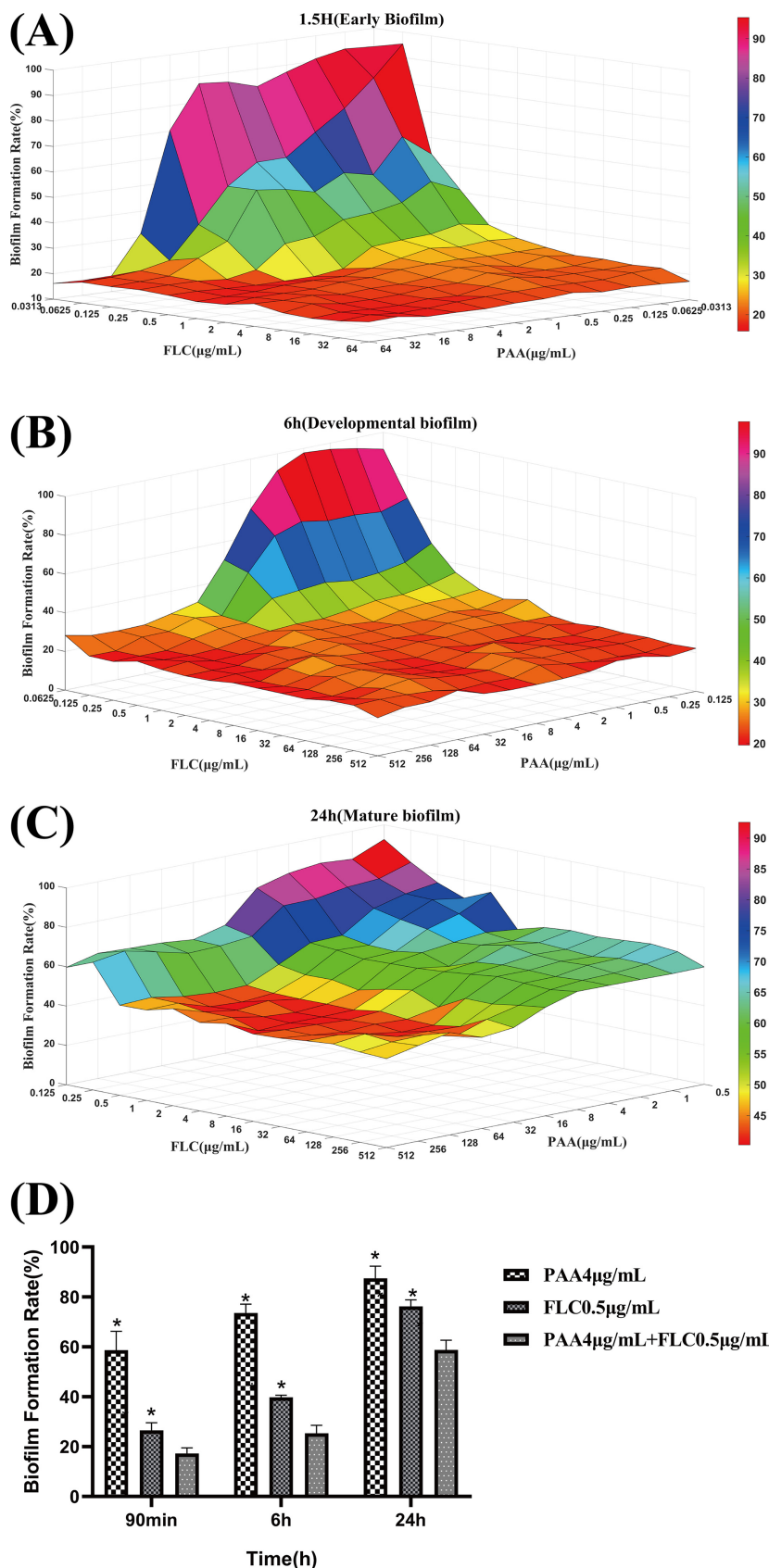


**FIG 2** Effect of PAA in combination with FLC against *C. albicans* biofilm formation at different formation stages. (A) Three-dimensional shaded surface figure of the effect of PAA combined with  
(Continued on next page)

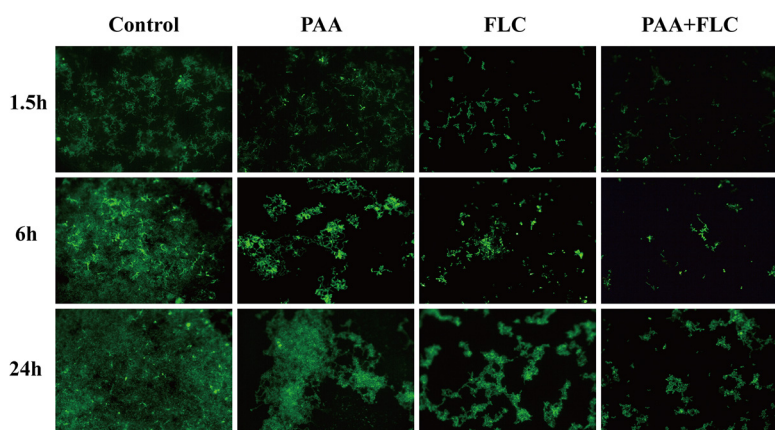


**FIG 3** Effect of PAA in combination with FLC on the growth and metabolic activity within the biofilm at different stages ( $\times 200$  magnification). Adhered biofilm cells were stained with FDA and visualized under a fluorescence microscope. Drug treatments: control (without PAA and FLC), PAA ( $4 \mu\text{g/mL}$ ), FLC ( $0.5 \mu\text{g/mL}$ ), and the combination of PAA ( $4 \mu\text{g/mL}$ ) and FLC ( $0.5 \mu\text{g/mL}$ ).

The adhesion rates of *C. albicans* treated with PAA ( $4 \mu\text{g/mL}$ ) or FLC ( $0.5 \mu\text{g/mL}$ ) alone were 76% and 62%, respectively, while the adhesion rate with the combination of PAA ( $4 \mu\text{g/mL}$ ) and FLC ( $0.5 \mu\text{g/mL}$ ) was 44%, which was notably lower than that of PAA alone ( $P < 0.001$ ) or FLC alone ( $P < 0.01$ ) (Fig. 4). This indicates that the combination of PAA and FLC remarkably reduced the adhesion strength of *C. albicans* during biofilm formation.

**(ii) PAA combined with FLC inhibited yeast-to-hypha transition of *C. albicans* during biofilm formation.** The yeast-to-hypha transition of *C. albicans* is an important aspect of biofilm development and maintenance (15). *C. albicans* hyphae induced by spider medium (1% nutrient broth + 1% D-Mannitol + 0.2% dipotassium hydrogen phosphate) and yeast extract-peptone-dextrose medium with 10% fetal bovine serum (YPD–10% FBS) are displayed in Fig. 5. As shown, long and extensive hyphae formed a network in both spider medium and YPD–10% FBS. With increasing drug dosages, there was a dose-dependent inhibition effect of PAA on hypha formation in both media (Fig. 5A). Furthermore, when the drug concentration reached  $8 \mu\text{g/mL}$ , PAA shortened the length of hyphae and reduced yeast cell aggregates. The combination PAA-FLC treatment ( $4\text{-}\mu\text{g/mL}$  PAA +  $0.5\text{-}\mu\text{g/mL}$  FLC) greatly reduced the extent of yeast-to-hypha transition, with the presence of a few dispersed yeast cells. On the contrary, when PAA or FLC was used alone at the same concentration, longish hyphae and dense yeast cell aggregates were observed in the visual field (Fig. 5B). These results suggest that PAA in combination with FLC inhibited yeast-to-hypha transition and hypha formation, thereby inhibiting biofilm formation.

**(iii) PAA combined with FLC altered gene expression during biofilm formation.** The aforementioned experimental results demonstrate that PAA combined with FLC inhibits adhesion and yeast-to-hypha transition in *C. albicans*. To further investigate the underlying molecular mechanism, gene expression changes were observed under

#### FIG 2 Legend (Continued)

FLC against *C. albicans* biofilm formation at 1.5 h (early biofilm). (B) Three-dimensional shaded surface figure of the effect of PAA combined with FLC against *C. albicans* biofilm formation at 6 h (developmental biofilm). (C) Three-dimensional shaded surface figure of the effect of PAA combined with FLC against *C. albicans* biofilm formation at 24 h (mature biofilm). Three-dimensional surface plots are provided for the combination of PAA and FLC, in which the  $x$  and  $y$  axes indicate the concentrations of PAA and FLC, respectively, and the  $z$  axis represents the *C. albicans* biofilm formation rate. For the colored bar on the right, the closer to deep red the color is at the top of the bar, the less effective the drug combination against biofilm formation. (D) Effect of PAA ( $4 \mu\text{g/mL}$ ) or FLC ( $0.5 \mu\text{g/mL}$ ) alone on biofilm formation at specific stages (1.5, 6, and 24 h). Values represent the means  $\pm$  standard deviation of three replicates. \*,  $P < 0.05$  for the combination of PAA ( $4 \mu\text{g/mL}$ ) with FLC ( $0.5 \mu\text{g/mL}$ ) versus either drug alone.

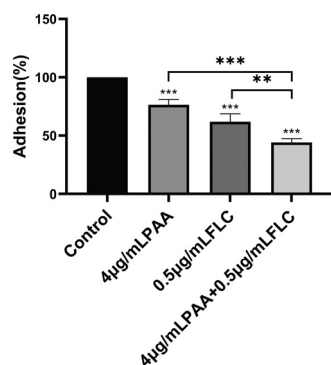
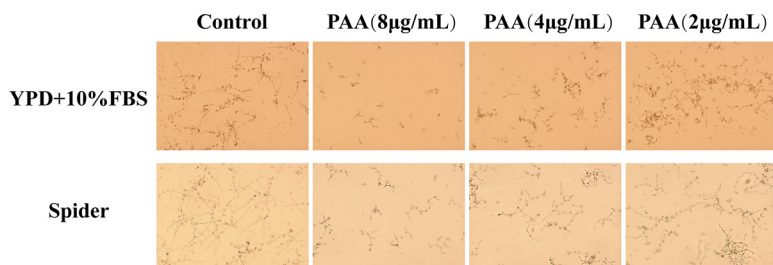


**FIG 4** Effect of PAA in combination with FLC on the adhesion of biofilms. The adhesion of biofilms treated with 4 µg/mL PAA, 0.5 µg/mL FLC, and 4 µg/mL PAA plus 0.5 µg/mL FLC was assayed. The data shown are the mean values  $\pm$  standard deviations from three independent experiments. \*,  $P < 0.05$ , \*\*,  $P < 0.01$ , and \*\*\*,  $P < 0.001$  compared with the control group; brackets indicate  $P$  values for the combination of PAA (4 µg/mL) and FLC (0.5 µg/mL) compared with either drug alone (one-way analysis of variance [ANOVA]).

this combination treatment. As shown by the results in Fig. 6A, the total transcriptomes of the four groups (control group, 4-µg/mL PAA group, 0.5-µg/mL FLC group, and 4-µg/mL PAA plus 0.5-µg/mL FLC combination group) were basically consistent. Notably, compared with the control group, a total of 1,725 significantly differentially expressed genes, including 1,403 upregulated and 322 downregulated genes, were observed in the PAA-FLC combination group ( $P < 0.05$ ), as shown in the volcano chart in Fig. 6B The Gene Ontology (GO) classification of genes in the combination treatment is shown in Fig. 6C. The differentially expressed genes were classified into 60 GO categories. Of these, 25 categories were associated with biological processes, 20 categories

(A)



(B)

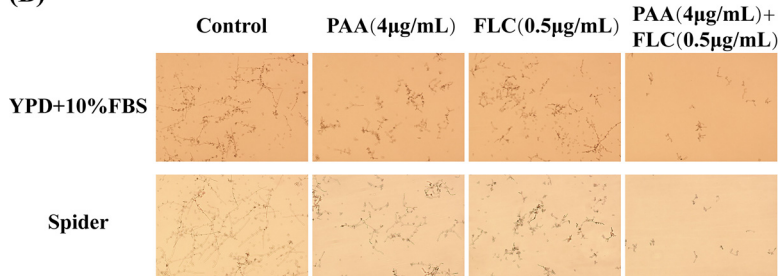


**FIG 5** Effect of PAA alone or in combination with FLC on yeast-to-hypha transition of *C. albicans* during biofilm formation in two different hypha-inducing media. (A) Effect of PAA alone on yeast-to-hypha transition of biofilm formation in spider or RPMI 1640 medium. PAA was diluted in spider or RPMI 1640 medium to final concentrations of 2, 4, and 8 µg/mL. Images were photographed at  $\times 20$  magnification. (B) Effect of PAA combined with FLC on yeast-to-hypha transition of biofilm formation in spider or RPMI 1640 medium. *C. albicans* ATCC 90028 cells were not treated (control; without PAA and FLC) and treated with PAA (4 µg/mL), FLC (0.5 µg/mL), and a combination of PAA (4 µg/mL) and FLC (0.5 µg/mL). Images were photographed at  $\times 100$  magnification.

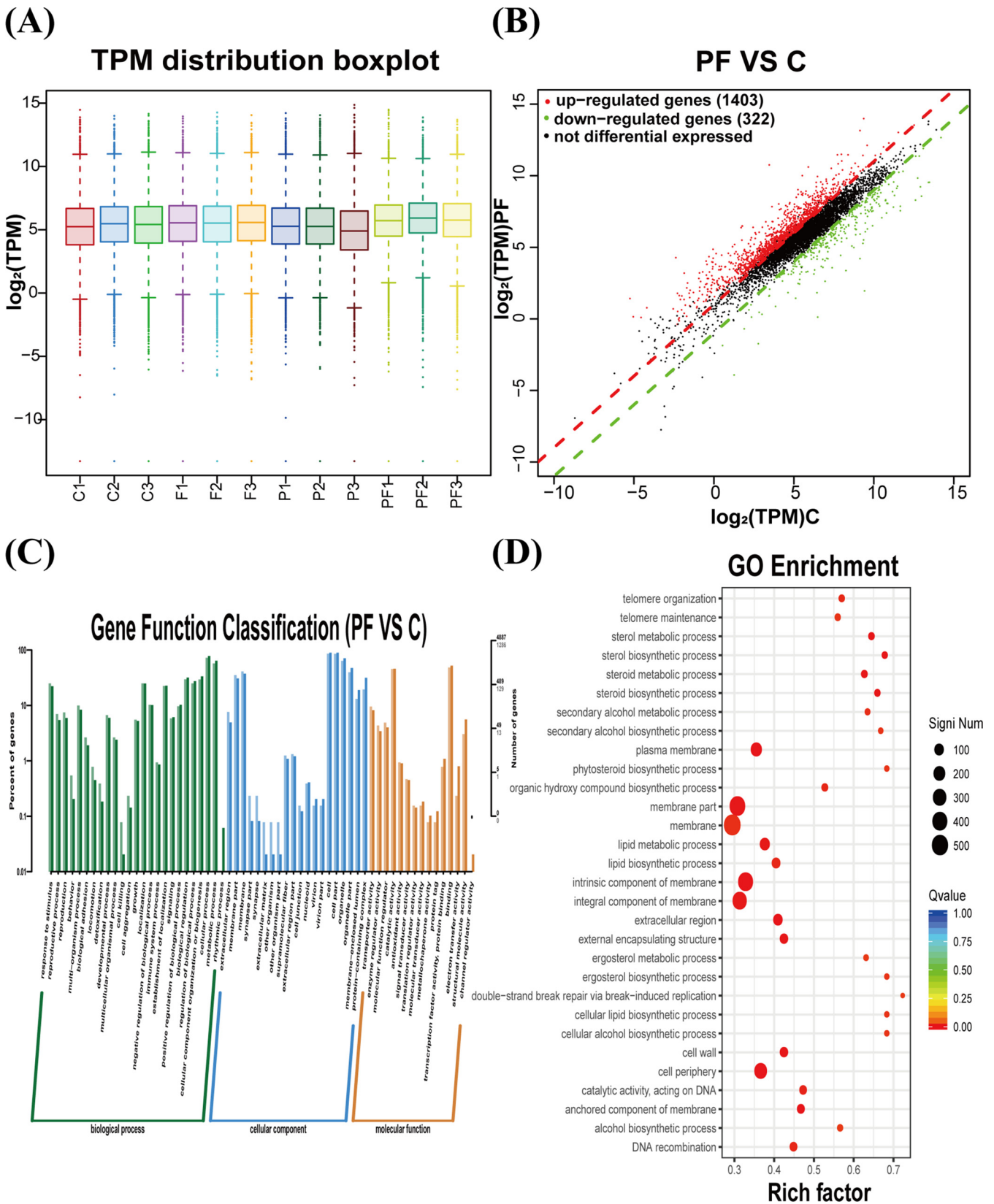


**FIG 6** Effect of PAA in combination with FLC on the transcriptome of *C. albicans* biofilms. (A) The abscissa is the sample name, and the ordinate is the  $\log_2(\text{TPM})$  value. TPM, transcripts per million. Box graphs for each region indicate five statistics (from top to bottom, maximum, upper quartile, median, lower quartile, and minimum). (B) The horizontal and vertical coordinates are the  $\log_2(\text{TPM})$  values of the PAA-FLC combination group (PF) and control (Continued on next page)

were associated with cellular components, and 15 categories were associated with molecular functions. Functional enrichment analysis of differentially expressed genes was also performed. Compared with the control group, most of the differentially expressed genes in the PAA-FLC combination group showed different degrees of functional enrichment. The top 30 GO terms with the highest enrichment ( $P < 0.05$ ) were selected (Fig. 6D). Through GO enrichment analysis, the differentially expressed genes were found to be enriched in functions related to double-strand break repair via break-induced replication, sterol biosynthetic process, sterol metabolic process, steroid metabolic process, steroid biosynthetic process, secondary alcohol biosynthetic process, secondary alcohol metabolic process, cellular lipid biosynthetic process, cellular alcohol biosynthetic process, phytosteroid biosynthetic process, ergosterol biosynthetic process, telomere organization, telomere maintenance, alcohol biosynthetic process, and organic hydroxy compound biosynthetic process (Rich factor of  $>0.5$ ).

Transcriptome sequencing (RNA-seq) analysis also revealed that the expression levels of genes involved in *C. albicans* biofilm formation were significantly altered under the combination treatment. To validate the RNA-seq results, four adhesion-associated genes (*ALS1*, *ALS2*, *ALS4*, and *SFP1*) and three hypha-associated genes (*ECE1*, *PRA1*, and *TEC1*) that were found to be related to biofilm formation in the quantitative reverse transcription PCR (qRT-PCR) experiment were selected. The combination treatment significantly altered the expression levels of adhesion-associated and hypha-associated genes, as listed in Table 1. The results presented in Fig. 7 show that PAA (4  $\mu\text{g/ml}$ ) treatment significantly downregulated the expression of *ALS4* in comparison to their expression in the control group ( $P < 0.001$ ) (Fig. 7). Increasing PAA concentrations produced more pronounced downregulation of gene expression. Although the expression of *ALS4* and *ALS2* decreased after FLC treatment, the PAA-FLC combination treatment downregulated the expression of *ALS4* and *ALS2* by 92% and 56% compared to their expression in the control group. Notably, the PAA-FLC combination treatment significantly downregulated the expression of *ALS1* compared with its expression with FLC treatment alone and in the untreated control group ( $P < 0.0001$ ), while the FLC treatment had no significant impact on *ALS1* expression compared with its expression in the control group ( $P > 0.05$ ). *ECE1*, *TEC1*, and *PRA1*, three important yeast-to-hypha transition regulators in *C. albicans* biofilm formation, were downregulated with the combination treatment in comparison to their expression in the untreated control group ( $P < 0.0001$ ) (Fig. 7). Furthermore, as the concentration of PAA increased, the expression levels of the three genes decreased ( $P < 0.01$ ) (Fig. 7). *SFP1*, the negative regulatory gene of *C. albicans* biofilm formation, was upregulated after the combination treatment compared with its expression in the control group ( $P < 0.0001$ ) (Fig. 7).

## DISCUSSION

*Candida albicans* is the most common cause of invasive candidiasis worldwide. Strong epidemiological evidence indicates that the mortality of invasive candidiasis is associated with biofilm formation (16, 17). Evidence suggests that *C. albicans* is more likely to form biofilms than other *Candida* species (such as *Candida tropicalis* and *Candida glabrata*) (18). *C. albicans* biofilms are dynamic and highly structured three-dimensional networks composed of a large number of hyphae and extracellular matrix. These biofilms are resistant to currently available antifungal drugs, especially azoles (19). Compared with planktonic cells, biofilms are up to 1,000 times more resistant to azoles (20). Therefore, in order to decrease the resistance of *C. albicans* to azole drugs, there is a critical need to identify new effective drugs or treatments that inhibit biofilm formation.

### FIG 6 Legend (Continued)

group (C), respectively. (C) The horizontal axis is the functional category, and the vertical axis is the number of genes in the category (right), annotated with its percentage of the total number of genes (left). (D) The vertical axis represents the function annotation information, and the horizontal axis represents the Rich factor corresponding to the function. The Rich factor is the number of differentially expressed genes annotated to that function divided by the number of genes annotated to that function (only the top 30 GO terms with the highest enrichment degree are presented).

**TABLE 1** Changes in important gene expression related to adhesion or filamentation in *C. albicans* biofilms after PAA and FLC treatment compared to the control group determined using RNA-seq

Value for indicated treatment in comparison to control <sup>a</sup>											
Gene identifier	Gene	FLC			PAA-FLC			PAA			
		Log <sub>2</sub> fold change	P value	Significant	Log <sub>2</sub> fold change	P value	Significant	Log <sub>2</sub> fold change	P value	Significant	
CAALFM_C603700WA	ALS1	0.465	0.356149125	No	-2.005	1.26913E-12	Yes	-0.995	0.024035599	Yes	
CAALFM_C604380WA	ALS2	-1.894	9.69431E-31	Yes	-1.831	7.89165E-17	Yes	-0.662	0.010456913	Yes	
CAALFM_C604130CA	ALS4	-2.576	8.71997E-38	Yes	-2.349	9.03704E-19	Yes	-0.681	0.005254679	Yes	
CAALFM_C403470CA	ECE1	-3.978	1.02707E-07	Yes	-3.657	2.99322E-08	Yes	-1.245	0.109592232	No	
CAALFM_C304530CA	TEC1	0.678	0.021587397	Yes	-0.916	2.24911E-06	Yes	-0.898	0.001729008	Yes	
CAALFM_C406980WA	PRA1	-4.359	6.55329E-15	Yes	-3.835	3.44915E-30	Yes	-1.085	0.355181787	No	
CAALFM_C304860WA	SFP1	0.399	0.079494286	No	1.269	3.65278E-05	Yes	-0.204	0.785353668	No	

<sup>a</sup>Log<sub>2</sub> fold change values were obtained from RNA-seq results.

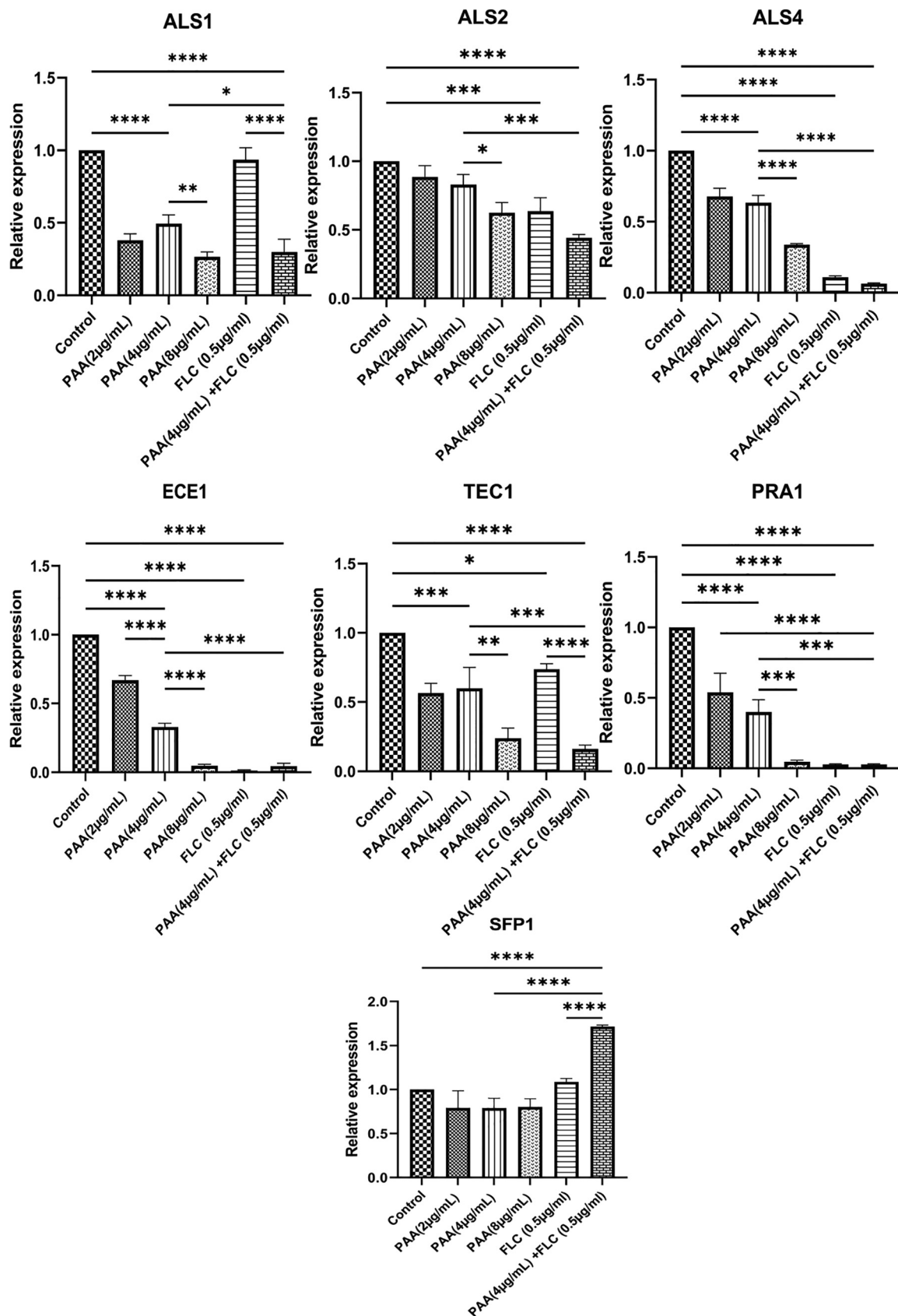


**FIG 7** Changes in gene expression related to biofilm formation after PAA and FLC treatment. *C. albicans* 90028 biofilms were treated with PAA (4 μg/mL) plus FLC (0.5 μg/mL), FLC (0.5 μg/mL), PAA (4 μg/mL), PAA (8 μg/mL), PAA (2 μg/mL), and RPMI 1640 medium (Continued on next page)

The pine bark of *Pseudolarix kaempferi* is a traditional Chinese medicine that has long been used to treat the dermatomycosis caused by microbe infection (21). Pseudolaric acid A (PAA) is a diterpenoid mainly derived from the pine bark of *Pseudolarix kaempferi*; it has a certain inhibitory effect on *C. albicans*. However, few published studies have investigated the effect of PAA alone or in combination with fluconazole (FLC) against *C. albicans* biofilm formation. In this study, we evaluated the inhibitory effect of PAA alone or in combination with FLC against *C. albicans* biofilm formation *in vitro*.

The formation of *C. albicans* biofilms involves several specific stages, including the early, developmental, and mature phases (14). In the present study, we observed a significant synergistic effect of PAA in combination with FLC against *C. albicans* biofilm formation. Changes in the fluorescence intensity of the fluorescein diacetate (FDA) assay further confirmed that PAA in combination with FLC significantly decreased the metabolic activity and growth of biofilm cells. The antibiofilm activity of PAA-FLC was stronger than that of PAA or FLC alone. Interestingly, the antibiofilm effect was mainly related to the dose of PAA in the mature biofilm phase, while the antibiofilm effect was primarily correlated with the concentration of FLC in the early and developmental phases of biofilm formation. We hypothesize that the reason for this may be that the synergistic antibiofilm effect of PAA and FLC probably involves different antifungal targets. Terpenoids can lead to membrane damage and respiratory chain dysfunction in *C. albicans* cells, which affects biofilm formation (22). The specific antibiofilm mechanism remains to be further studied, although PAA is a diterpenoid.

Cell adherence is the first step in biofilm formation. After the adhesion of *C. albicans* cells, the yeast cells gradually transform into hyphal forms, which is important not only for biofilm development but also for biofilm dissemination (23). Adhesion and yeast-to-hypha transition are considered the crucial pathogenic elements. Inhibition of adhesion or yeast-to-hypha transition can induce biofilm formation defects, which is a novel target for biofilm-specific treatment (24, 25). Our data showed that the PAA-FLC combination treatment not only inhibited adhesion effectively but also suppressed yeast-to-hypha transition. The inhibition of adhesion and yeast-to-hypha transition in the combination treatment (PAA-FLC) was stronger than that produced by the individual drugs. The synergistic antibiofilm action of the PAA-FLC combination was likely due to inhibition of adhesion and yeast-to-hypha transition.

To investigate the synergistic antibiofilm mechanisms of PAA combined with FLC, RNA-seq and qRT-PCR were used to analyze changes at the transcriptional and genetic levels. Both independent trials indicated that the combined use of PAA and FLC effectively altered the expression of *ALS1*, *ALS4*, *ALS2*, *SFP1*, *ECE1*, *TEC1*, and *PRA1*. The *ALS* family, including *ALS1*, *ALS2*, and *ALS4*, contributes to the adhesion and aggregation of yeast cells and is an integral part of biofilm formation (26). *SFP1* is one of the few negative regulators of adhesion, and the deletion of *SFP1* results in the promotion of biofilm formation (27). *ECE1* is a hyphal induction gene that stimulates hypha formation and elongation (28). *TEC1* and *PRA1*, the master regulatory genes involved in biofilm formation, play crucial roles in hyphal development (29, 30). Notably, *TEC1* is important for regulating the morphological switch between yeast and hypha (31). The aforementioned phenotypic results indicate that the PAA-FLC combination had a strong effect on the inhibition of adhesion and yeast-to-hypha transition during biofilm formation. The PAA-FLC combination treatment downregulated the expression of adhesion-related genes (*ALS4*, *ALS2*, and *ALS1*) and hypha-related genes (*ECE1*, *TEC1*, and *PRA1*) during biofilm formation. At the same time, the PAA-FLC combination treatment remarkably increased the expression of the negative-regulation gene (*SFP1*). The genotypic and phenotypic results were correlated. PAA and FLC may have various antibiofilm targets,

#### FIG 7 Legend (Continued)

(control). Gene expression was measured by qRT-PCR. qRT-PCR was independently repeated three times, with two technical replicates in each experiment. Data represent the mean values  $\pm$  standard deviations from three triplicate experiments. *P* values were determined by ANOVA. \*, *P* < 0.05; \*\*, *P* < 0.01; \*\*\*, *P* < 0.001; \*\*\*\*, *P* < 0.0001.

which contributes to their synergistic effect. Both PAA and FLC alone had certain inhibitory effects on the gene expression of *ALS2*, *ALS4*, *ECE1*, and *PRA1*. However, PAA in combination with FLC produced more significant inhibitory effects on these genes compared to either of the drugs alone. Notably, PAA, rather than FLC, may have a primary role in suppressing the expression of *ALS1*. These findings reveal the deep mechanism underlying the synergistic inhibition of *C. albicans* biofilm formation by PAA in combination with FLC.

In conclusion, the present study demonstrates, for the first time, the antibiofilm effect of PAA alone and in combination with FLC on *C. albicans*. PAA exhibited better synergistic inhibitory effects on *C. albicans* biofilm formation when combined with FLC. Furthermore, PAA in combination with FLC inhibited adhesion and hyphal morphogenesis during biofilm formation. Moreover, PAA-FLC combination treatment not only specifically inhibited adhesion- and hypha-related genes but also increased the expression of the gene that negatively regulates biofilm formation. These results provide novel insights into the synergistic effect and mechanisms of PAA, a traditional Chinese medicine, combined with antifungal drugs.

## MATERIALS AND METHODS

**Strains, growth conditions, and reagents.** The reference strain *C. albicans* ATCC 90028 was used in all experiments. *C. albicans* ATCC 90028 was preserved in a medium containing 20% glycerol at  $-80^{\circ}\text{C}$ . The strain was subcultured twice on Sabouraud agar plate medium (Comagal Microbial Technology Co., Shanghai, China) for 16 h at  $37^{\circ}\text{C}$  before each experiment. PAA was obtained from Tauto Biotech Co., Ltd. (Shanghai, China). FLC with a purity of  $>98\%$  was purchased from Sigma-Aldrich. Both PAA and FLC were dissolved in dimethyl sulfoxide (DMSO); the final concentration of DMSO was lower than 0.1%. In addition, RPMI 1640 was obtained from Fisher Scientific. MOPS [3-(*N*-morpholino) propanesulfonic acid] was obtained from Sangon Biotech, Shanghai. Tetrazolium {XTT [2,3-bis-(2-methoxy-4-nitro-5-sulphophenyl)-2H-tetrazolium-5-carboxanilide salt]} and fluorescein diacetate were purchased from Sigma-Aldrich.

**Antibiofilm formation. (i) XTT reduction assay.** The effects on biofilm formation of PAA or FLC alone and in combination were determined by XTT reduction assays (32, 33). Biofilms were generated on commercial polystyrene 6-well microtiter plates. In brief,  $100\ \mu\text{L}$  of *C. albicans* ATCC 90028 (about  $1.5 \times 10^6$  CFU/mL) in RPMI 1640 medium was seeded into 96-well plates for biofilm formation. At different phases of biofilm formation (1.5, 6, or 24 h), the medium and planktonic cells in each well were removed and washed with phosphate-buffered saline (PBS). Then,  $100\ \mu\text{L}$  of RPMI 1640 medium containing PAA or FLC was added to each well. In terms of the antibiofilm activity of the combination treatment,  $50\ \mu\text{L}$  of RPMI 1640 medium containing PAA alone (or FLC) was placed in each well at planned time points based on the microdilution checkerboard approach. After the plates were incubated at  $37^{\circ}\text{C}$  for 24 h, the biofilm in each well was washed gently three times with  $100\ \mu\text{L}$  PBS to remove the planktonic cells. A cell proliferation kit II (XTT; Sigma-Aldrich) was used to evaluate the effect of biofilm formation. XTT and electron coupling reagent were mixed at 50:1 (vol/vol) immediately prior to the assay. Afterwards, PBS was added to the XTT mixture (1.96:1, vol/vol) and  $151\ \mu\text{L}$  of this mixture was placed into each well. Then, the plates were incubated in the dark for 2 h at  $37^{\circ}\text{C}$ . The colored supernatants were transferred to new 96-well plates, and the optical density at 492 nm ( $\text{OD}_{492}$ ) was measured. Each experiment was performed in triplicate.

**(ii) FDA assay.** A fluorescein diacetate (FDA) assay was used to quantify the viable biofilm biomass (34, 35). In brief, *C. albicans* ATCC 90028 (about  $1.5 \times 10^6$  CFU/mL) in RPMI 1640 medium was transferred into 6-well plates for biofilm formation. After incubation (1.5, 6, or 24 h), planktonic cells were removed, and the biofilms were left untreated or were treated with  $4\ \mu\text{g/mL}$  PAA,  $0.5\ \mu\text{g/mL}$  FLC, or  $4\ \mu\text{g/mL}$  PAA in combination with  $0.5\ \mu\text{g/mL}$  FLC for 24 h at  $37^{\circ}\text{C}$ . Each well was washed with PBS three times to remove the planktonic cells. Next,  $0.2\ \text{mg/mL}$  of FDA (Sigma-Aldrich, Shanghai, China) and fresh RPMI 1640 medium were mixed 1:1 (vol/vol) immediately prior to the assay. The FDA mixture was then transferred into each pre-rinsed well. The 6-well plates were incubated at  $37^{\circ}\text{C}$  for 1 h in the dark. Before observation, the plates were gently rinsed with PBS two times to remove the dye residue. The morphology of the biofilms was observed under a fluorescence microscope (EUROStar III plus; Ou Meng, Germany) at  $\times 200$  magnification.

**(iii) Cell adhesion assay.** The *in vitro* cell adherence assay was performed according to previously reported methods, with some modifications (36, 37). An overnight culture of *C. albicans* ATCC 90028 was adjusted in RPMI 1640 medium to a final concentration of about  $1.5 \times 10^6$  CFU/mL. Amounts of  $200\ \mu\text{L}$  of cell suspensions were inoculated into the wells of a 96-well plate and PAA ( $4\ \mu\text{g/mL}$ ), FLC ( $0.5\ \mu\text{g/mL}$ ), or the combination of the two was added to the cell suspensions. *C. albicans* cell suspensions without medication were regarded as the control. After the plates were incubated at  $37^{\circ}\text{C}$  for 3 h, the liquid medium was thrown away. Each well containing cells was washed three times. Then, the XTT mixture with PBS, as described above, was added to each well, and the cells were incubated in the dark for 2 h at  $37^{\circ}\text{C}$ . The supernatants obtained were transferred to a new 96-well plate and the  $\text{OD}_{492}$  was analyzed. The relative adhesion rate of *C. albicans* cells was expressed as follows: adhesion rate = ( $\text{OD}_{492}$  of treatment/ $\text{OD}_{492}$  of negative control)  $\times 100\%$  (38). Each experiment was carried out in triplicate.

**TABLE 2** Primer sequences used for qRT-PCR in the study

Primer	Sequence (5'–3')	Length (bp)	Reference or source
ACT1-Forward	TCAGACCAGCTGATTTAGGTTTG	23	41
ACT1-Reverse	GTGAACAATGGATGGACCAG	20	41
ALS1-Forward	TTGGGTTGGTCCTTAGATGG	20	42
ALS1-Reverse	ATGATTCAAAGCGTCGTTC	19	42
ALS2-Forward	TGGTGAATGGGGTTCATAGT	21	43
ALS2-Reverse	CGATAACCAGCGGGGACAT	19	43
ALS4-Forward	TCCGAGTCCATTCCAGTACTAA	22	44
ALS4-Reverse	GTTACAGCATCACTAGAAGGAATATC	26	44
ECE1-Forward	GCTGGTATCATTGCTGATAT	20	42
ECE1-Reverse	TTCGATGGATTGTTGAACAC	20	42
TEC1-Forward	TCAACAGTCACGAGGAA	17	45
TEC1-Reverse	TGGCTGGGAGATGC	14	45
PRA1-Forward	GGCGAAGGGTGAATGGAGATG	22	This study
PRA1-Reverse	GAGAACTTGAGGCTGTGCTACTGG	24	This study
SFP1-Forward	GCACGTCACCTCTACGTTATGG	22	This study
SFP1-Reverse	CGATGACCGGGCACTTG	17	This study

**Yeast-to-hypha transition assay.** The effect of PAA alone and in combination with FLC on the yeast-to-hypha phase transition of *C. albicans* was measured according to previously described methods, with minor alterations (39, 40). *C. albicans* ATCC 90028 was incubated overnight in YPD medium. Then, the fungal supernatant (about  $1.5 \times 10^5$  CFU/mL) with PAA (at 4  $\mu$ g/mL), FLC (0.5  $\mu$ g/mL), or the combination of the two was incubated in YPD–10% FBS or spider medium at 37°C for 6 h. The fungal supernatant without drug treatment served as the control. Samples were incubated under aerobic conditions with continuous shaking at 120 rpm. After 6 h of incubation, 20  $\mu$ L of cell suspension was transferred to a fast counter plate to observe the yeast cells and hyphae form under a light microscope with a  $\times 10$  magnification eyepiece and 10 $\times$  lens objective.

**RNA-seq analysis of *C. albicans* biofilms.** First, 1.5 mL of *C. albicans* ATCC 90028 (about  $1.5 \times 10^6$  CFU/mL) in RPMI 1640 medium was seeded into 6-well polystyrene plates and cultured at 37°C for 1.5 h. After 1.5 h of incubation for biofilm formation, 1.5 mL of RPMI 1640 medium containing PAA (4  $\mu$ g/mL), FLC (0.5  $\mu$ g/mL), or the combination of the two was added to each well, and the plates were incubated for a further 24 h at 37°C. The control wells were free of FLC and PAA. Then, the biofilms were gently washed three times with PBS and collected with a sterile cell scraper. Total RNA from the *C. albicans* biofilms was extracted by using a nucleic acid purification kit (MagExtractor; Toyobo Co., Ltd., Osaka, Japan) following the manufacturer's instructions; genomic DNA contamination was removed using RNase-free DNase I (Toyobo). The quality and quantity of RNA samples were checked using a Qubit RNA assay kit (Life Technologies, CA, USA) before RNA sequencing. High-quality RNA samples were sent to Sangon Biotech company, Shanghai, China, for library preparation and sequencing. The sequencing libraries were prepared using the VAHTS mRNA-seq version 2 library prep kit for Illumina according to the manufacturer's protocols, and sequencing was performed on a NovaSeq 6000 sequencer (Illumina, Inc., USA). The quality of the RNA sequencing data was analyzed using FastQC (<http://www.bioinformatics.babraham.ac.uk/projects/fastqc/>). The raw data were quality filtered using Trimmomatic (TRAILING: 30) to obtain relatively accurate and clean data. HISAT2 (version 2.0.1) was used to map the clean reads to the reference genome and the alignment results were counted using RSeQC (version 2.6.1). The expression of genes was quantified using StringTie (version 1.3.3), and differential analysis of gene expression was carried out using DESeq2 (version 1.20.0). Gene Ontology (GO) enrichment analysis was carried out using the topGO R package in order to acquire the gene functions of differentially expressed genes. The experiments were repeated in triplicate with independent trials.

**Specific gene expression related to biofilm formation by qRT-PCR.** *C. albicans* suspensions (ATCC 90028) with a cell density of about  $1.5 \times 10^6$  CFU/mL were seeded into 6-well polystyrene plates and cultured at 37°C for 1.5 h. After 1.5 h of incubation, PAA (2  $\mu$ g/mL), PAA (4  $\mu$ g/mL), PAA (8  $\mu$ g/mL), FLC (0.5  $\mu$ g/mL), or PAA (4  $\mu$ g/mL) plus FLC (0.5  $\mu$ g/mL) was added, and the plates were incubated for a further 24 h at 37°C. The biofilms were gently washed three times with PBS and collected with a sterile cell scraper. Total RNA from the *C. albicans* biofilms was extracted with a nucleic acid purification kit (MagExtractor, Toyobo Co., Ltd., Osaka, Japan) according to the manufacturer's instructions. Then, about 1  $\mu$ g of total RNA was treated with a RevertAid first-strand cDNA synthesis kit (Thermo Scientific, Inc.) and was reverse transcribed at 42°C for 1 h and 70°C for 5 min. qRT-PCRs were carried out using SYBR green real-time PCR master mix (Toyobo Co., Ltd., Osaka, Japan) on a Bio-Rad CFX96 real-time system (Bio-Rad). Each reaction mixture volume (25  $\mu$ L) contained 12.5  $\mu$ L of SYBR green master mix, 1  $\mu$ L of cDNA, 1  $\mu$ L of forward primer, 1  $\mu$ L of reverse primer, and 9.5  $\mu$ L of distilled water. Primers for *C. albicans* biofilms were designed and synthesized by BioSune Biotechnology Co., Ltd. (Shanghai, China). The primer sequences used to amplify gene segments are shown in Table 2. For qRT-PCR, the thermal cycling conditions were as follows: 95°C for 60 s, followed by 40 cycles at 95°C for 10 s, annealing at 60°C for 15 s, and extension at 72°C for 45 s. After qRT-PCR, melting curve analysis was carried out to check for non-specific amplification. The target gene expression was calculated by the  $2^{-\Delta\Delta C_T}$  cycle threshold ( $C_T$ ) method using the *ACT* gene as the internal reference gene; the  $\Delta C_T$  value was expressed as the average

$C_T$  value for the target gene minus the average  $C_T$  value for *ACT*. qRT-PCR assays for each gene were performed in triplicate.

**Statistical analysis.** Graphs and statistical analyses were performed with GraphPad Prism 9 (GraphPad software, Inc.). Differences among three or more groups were evaluated by analysis of variance (ANOVA), while intergroup differences were further determined using the Bonferroni method. *P* values less than 0.05 (\*, *P* < 0.05, \*\*, *P* < 0.01, \*\*\*, *P* < 0.001, \*\*\*\*, *P* < 0.0001) were considered as statistically significant.

**Data availability.** The RNA-seq data from this study have been deposited in the NCBI database under the BioProject accession number [PRJNA757949](https://www.ncbi.nlm.nih.gov/bioproject/PRJNA757949).

## SUPPLEMENTAL MATERIAL

Supplemental material is available online only.

**SUPPLEMENTAL FILE 1**, PDF file, 0.2 MB.

## ACKNOWLEDGMENTS

This work was financially supported by the National Natural Science Youth Foundation of China (grant number 82003817), Longhua Innovation Project (grant number CX202058), and Shanghai Rising Stars of Medical Talent Youth Development Program [grant number SHWRS (2018)-02].

We have no conflicts of interest.

## REFERENCES

- Brown GD, Denning DW, Gow NA, Levitz SM, Netea MG, White TC. 2012. Hidden killers: human fungal infections. *Sci Transl Med* 4:165rv13. <https://doi.org/10.1126/scitranslmed.3004404>.
- Pitarch A, Nombela C, Gil C. 2018. Diagnosis of invasive candidiasis: from gold standard methods to promising leading-edge technologies. *Curr Top Med Chem* 18:1375–1392. <https://doi.org/10.2174/1568026618666181025093146>.
- Pappas PG, Lionakis MS, Arendrup MC, Ostrosky-Zeichner L, Kullberg BJ. 2018. Invasive candidiasis. *Nat Rev Dis Primers* 4:18026. <https://doi.org/10.1038/nrdp.2018.26>.
- Mayer FL, Wilson D, Hube B. 2013. *Candida albicans* pathogenicity mechanisms. *Virulence* 4:119–128. <https://doi.org/10.4161/viru.22913>.
- Allen D, Wilson D, Drew R, Perfect J. 2015. Azole antifungals: 35 years of invasive fungal infection management. *Expert Rev Anti Infect Ther* 13:787–798. <https://doi.org/10.1586/14787210.2015.1032939>.
- Hoehamer CF, Cummings ED, Hilliard GM, Rogers PD. 2010. Changes in the proteome of *Candida albicans* in response to azole, polyene, and echinocandin antifungal agents. *Antimicrob Agents Chemother* 54:1655–1664. <https://doi.org/10.1128/AAC.00756-09>.
- Marak MB, Dhanashree B. 2018. Antifungal susceptibility and biofilm production of *Candida* spp. isolated from clinical samples. *Int J Microbiol* 2018:7495218. <https://doi.org/10.1155/2018/7495218>.
- Newman DJ, Cragg GM. 2020. Natural products as sources of new drugs over the nearly four decades from 01/1981 to 09/2019. *J Nat Prod* 83:770–803. <https://doi.org/10.1021/acs.jnatprod.9b01285>.
- Khan MS, Ahmad I. 2012. Antibiofilm activity of certain phytocompounds and their synergy with fluconazole against *Candida albicans* biofilms. *J Antimicrob Chemother* 67:618–621. <https://doi.org/10.1093/jac/dkr512>.
- Dong HH, Wang YH, Peng XM, Zhou HY, Zhao F, Jiang YY, Zhang DZ, Jin YS. 2021. Synergistic antifungal effects of curcumin derivatives as fungal biofilm inhibitors with fluconazole. *Chem Biol Drug Des* 97:1079–1088. <https://doi.org/10.1111/cbdd.13827>.
- Zhou BN. 1991. Some progress on the chemistry of natural bioactive terpenoids from Chinese medicinal plants. *Mem Inst Oswaldo Cruz* 86(Suppl 2):219–226. <https://doi.org/10.1590/s0074-02761991000600049>.
- Chiu P, Leung LT, Ko BC. 2010. Pseudolaric acids: isolation, bioactivity and synthetic studies. *Nat Prod Rep* 27:1066–1083. <https://doi.org/10.1039/b906520m>.
- Penesyan A, Paulsen IT, Gillings MR, Kjelleberg S, Manefield MJ. 2020. Secondary effects of antibiotics on microbial biofilms. *Front Microbiol* 11:2109. <https://doi.org/10.3389/fmicb.2020.02109>.
- Soll DR, Daniels KJ. 2016. Plasticity of *Candida albicans* biofilms. *Microbiol Mol Biol Rev* 80:565–595. <https://doi.org/10.1128/MMBR.00068-15>.
- Gulati M, Nobile CJ. 2016. *Candida albicans* biofilms: development, regulation, and molecular mechanisms. *Microbes Infect* 18:310–321. <https://doi.org/10.1016/j.micinf.2016.01.002>.
- Rodrigues LS, Motta FA, Picharski GL, Vasconcelos TM, Riccieri MC, Dalla-Costa LM. 2019. Invasive candidiasis: risk factor for mortality in a pediatric tertiary care hospital in south of Brazil. *Medicine (Baltimore)* 98:e15933. <https://doi.org/10.1097/MD.00000000000015933>.
- Lee CH, Chen YC, Chen IL, Chen FJ, Chien CC. 2020. Impact of biofilm production by *Candida* species and antifungal therapy on mortality of patients with candidemia. *Mycoses* 63:1382–1391. <https://doi.org/10.1111/myc.13179>.
- Brunetti G, Navazio AS, Giuliani A, Giordano A, Proli EM, Antonelli G, Raponi G. 2019. *Candida* blood stream infections observed between 2011 and 2016 in a large Italian university hospital: a time-based retrospective analysis on epidemiology, biofilm production, antifungal agents consumption and drug-susceptibility. *PLoS One* 14:e0224678. <https://doi.org/10.1371/journal.pone.0224678>.
- Wall G, Montelongo-Jauregui D, Vidal Bonifacio B, Lopez-Ribot JL, Uppuluri P. 2019. *Candida albicans* biofilm growth and dispersal: contributions to pathogenesis. *Curr Opin Microbiol* 52:1–6. <https://doi.org/10.1016/j.mib.2019.04.001>.
- de Barros PP, Rossoni RD, de Souza CM, Scorzoni L, Fenley JC, Junqueira JC. 2020. *Candida* biofilms: an update on developmental mechanisms and therapeutic challenges. *Mycopathologia* 185:415–424. <https://doi.org/10.1007/s11046-020-00445-w>.
- He WJ, Chu HB, Zhang YM, Han HJ, Yan H, Zeng GZ, Fu ZH, Olubanke O, Tan NH. 2011. Antimicrobial, cytotoxic lignans and terpenoids from the twigs of *Pseudolarix kaempferi*. *Planta Med* 77:1924–1931. <https://doi.org/10.1055/s-0031-1280020>.
- Touil HFZ, Boucherit K, Boucherit-Otmani Z, Kohder G, Madkour M, Soliman SSM. 2020. Optimum inhibition of amphotericin-B-resistant *Candida albicans* strain in single- and mixed-species biofilms by *Candida* and non-*Candida* terpenoids. *Biomolecules* 10:342. <https://doi.org/10.3390/biom10020342>.
- Li X, Hou Y, Yue L, Liu S, Du J, Sun S. 2015. Potential targets for antifungal drug discovery based on growth and virulence in *Candida albicans*. *Antimicrob Agents Chemother* 59:5885–5891. <https://doi.org/10.1128/AAC.00726-15>.
- Dwivedi M, Muralidhar S, Saluja D. 2020. Hibiscus sabdariffa extract inhibits adhesion, biofilm initiation and formation in *Candida albicans*. *Indian J Microbiol* 60:96–106. <https://doi.org/10.1007/s12088-019-00835-9>.
- Fazly A, Jain C, Dehner AC, Issi L, Lilly EA, Ali A, Cao H, Fidel PL, Jr, Rao RP, Kaufman PD. 2013. Chemical screening identifies filastatin, a small molecule inhibitor of *Candida albicans* adhesion, morphogenesis, and pathogenesis. *Proc Natl Acad Sci U S A* 110:13594–13599. <https://doi.org/10.1073/pnas.1305982110>.
- Nailis H, Kuchariková S, Rícicová M, Van Dijk P, Deforce D, Nelis H, Coenye T. 2010. Real-time PCR expression profiling of genes encoding potential virulence factors in *Candida albicans* biofilms: identification of model-dependent and -independent gene expression. *BMC Microbiol* 10:114. <https://doi.org/10.1186/1471-2180-10-114>.

27. Chen HF, Lan CY. 2015. Role of SFP1 in the regulation of *Candida albicans* biofilm formation. *PLoS One* 10:e0129903. <https://doi.org/10.1371/journal.pone.0129903>.
28. Engku Nasrullah Satiman EAF, Ahmad H, Ramzi AB, Abdul Wahab R, Kaderi MA, Wan Harun WHA, Dashper S, McCullough M, Arzmi MH. 2020. The role of *Candida albicans* candidalysin ECE1 gene in oral carcinogenesis. *J Oral Pathol Med* 49:835–841. <https://doi.org/10.1111/jop.13014>.
29. Daniels KJ, Srikantha T, Pujol C, Park YN, Soll DR. 2015. Role of Tec1 in the development, architecture, and integrity of sexual biofilms of *Candida albicans*. *Eukaryot Cell* 14:228–240. <https://doi.org/10.1128/EC.00224-14>.
30. Kurakado S, Arai R, Sugita T. 2018. Association of the hypha-related protein Pra1 and zinc transporter Zrt1 with biofilm formation by the pathogenic yeast *Candida albicans*. *Microbiol Immunol* 62:405–410. <https://doi.org/10.1111/1348-0421.12596>.
31. Villa S, Hamideh M, Weinstock A, Qasim MN, Hazbun TR, Sellam A, Hernday AD, Thangamani S. 2020. Transcriptional control of hyphal morphogenesis in *Candida albicans*. *FEMS Yeast Res* 20:foaa005. <https://doi.org/10.1093/femsyr/foaa005>.
32. Manoharan RK, Lee JH, Kim YG, Lee J. 2017. Alizarin and chrysin inhibit biofilm and hyphal formation by *Candida albicans*. *Front Cell Infect Microbiol* 7:447. <https://doi.org/10.3389/fcimb.2017.00447>.
33. Ramage G, Vande Walle K, Wickes BL, López-Ribot JL. 2001. Standardized method for in vitro antifungal susceptibility testing of *Candida albicans* biofilms. *Antimicrob Agents Chemother* 45:2475–2479. <https://doi.org/10.1128/AAC.45.9.2475-2479.2001>.
34. Peeters E, Nelis HJ, Coenye T. 2008. Comparison of multiple methods for quantification of microbial biofilms grown in microtiter plates. *J Microbiol Methods* 72:157–165. <https://doi.org/10.1016/j.mimet.2007.11.010>.
35. Różalska B, Sadowska B, Budzyńska A, Bernat P, Różalska S. 2018. Biogenic nanosilver synthesized in *Metarhizium robertsii* waste mycelium extract—as a modulator of *Candida albicans* morphogenesis, membrane lipidome and biofilm. *PLoS One* 13:e0194254. <https://doi.org/10.1371/journal.pone.0194254>.
36. Dutreix L, Bernard C, Juin C, Imbert C, Girardot M. 2018. Do raspberry extracts and fractions have antifungal or anti-adherent potential against *Candida* spp.? *Int J Antimicrob Agents* 52:947–953. <https://doi.org/10.1016/j.ijantimicag.2018.08.020>.
37. Wady AF, Machado AL, Zucolotto V, Zamperini CA, Berni E, Vergani CE. 2012. Evaluation of *Candida albicans* adhesion and biofilm formation on a denture base acrylic resin containing silver nanoparticles. *J Appl Microbiol* 112:1163–1172. <https://doi.org/10.1111/j.1365-2672.2012.05293.x>.
38. Wijesinghe GK, Maia FC, de Oliveira TR, de Feiria SNB, Joia F, Barbosa JP, Boni GC, Sardi JCO, Rosalen PL, Höfling JF. 2020. Effect of *Cinnamomum verum* leaf essential oil on virulence factors of *Candida* species and determination of the in-vivo toxicity with *Galleria mellonella* model. *Mem Inst Oswaldo Cruz* 115:e200349. <https://doi.org/10.1590/0074-02760200349>.
39. Toenjes KA, Munsee SM, Ibrahim AS, Jeffrey R, Edwards JE, Jr, Johnson DL. 2005. Small-molecule inhibitors of the budded-to-hyphal-form transition in the pathogenic yeast *Candida albicans*. *Antimicrob Agents Chemother* 49:963–972. <https://doi.org/10.1128/AAC.49.3.963-972.2005>.
40. Priya A, Pandian SK. 2020. Piperine impedes biofilm formation and hyphal morphogenesis of *Candida albicans*. *Front Microbiol* 11:756. <https://doi.org/10.3389/fmicb.2020.00756>.
41. Böttcher B, Hoffmann B, Garbe E, Weise T, Cseresnyés Z, Brandt P, Dietrich S, Driesch D, Figge MT, Vylkova S. 2020. The transcription factor Stp2 is important for *Candida albicans* biofilm establishment and sustainability. *Front Microbiol* 11:794. <https://doi.org/10.3389/fmicb.2020.00794>.
42. Yan Y, Tan F, Miao H, Wang H, Cao Y. 2019. Effect of shikonin against *Candida albicans* biofilms. *Front Microbiol* 10:1085. <https://doi.org/10.3389/fmicb.2019.01085>.
43. Razavi T, Falahati M, Teimourian S, Farahyar S, Babaei V, Majdabadi N, Iraj E. 2020. Investigating the expression of ALS2 and ALS9 genes along with allele frequency of ALS9 in patients with vulvovaginal candidiasis. *Infect Genet Evol* 82:104253. <https://doi.org/10.1016/j.meegid.2020.104253>.
44. Hoyer LL, Payne TL, Hecht JE. 1998. Identification of *Candida albicans* ALS2 and ALS4 and localization of ALS proteins to the fungal cell surface. *J Bacteriol* 180:5334–5343. <https://doi.org/10.1128/JB.180.20.5334-5343.1998>.
45. Liu RH, Shang ZC, Li TX, Yang MH, Kong LY. 2017. In vitro antibiofilm activity of eucarobustol E against *Candida albicans*. *Antimicrob Agents Chemother* 61:e02707-16. <https://doi.org/10.1128/AAC.02707-16>.